Supporting Information

A 2D Dy-Based Metal−Organic Framework Derived from Benzothiadiazole: Structure and Photocatalytic Properties

Jing Zhu[a], Lin Hua[b], Yumeng Zhang[a], Hongying Wu[b], Fuwei Zheng[b], Hongyan Shen[b], Haiyan Gong[c,*], Liu Yang[b,*], Aiyun Jiang[a,*]

[a] Huanghe Science and Technology College, Zhengzhou, Henan 450063, China.

[b] Institute of Chemistry Co. Ltd Henan Academy of Sciences, Zhengzhou, 450002, P. R. China

[c] Academy of Chinese Medical Sciences, Henan University of Chinese Medicine，Zhengzhou 450046，Henan, China

*Correspondence Email: aiyunjiang@126.com, ghy_mz@163.com, 13937102338@139.com.

Table of Contents:

Supporting Tables	
Table S1	Crystallographic data of the complex MOL **1**.
Table S2	Selected bond lengths (Å) and angles (°) of complex MOL **1**.
Table S3	*SHAPE* analysis of the Dy1 ion in MOL **1**.
Table S4	Computed oxidation potential of chalcone.
Supporting Figures	
Scheme S1	A photo of the reactor under 30 W LED light.
Figure S1	The coordinated environment of Dy(III) ion.
Figure S2	a) n = 2, the *Tauc* plot of MOL **1**; b) n = 1/2, the *Tauc* plot of MOL **1**.
Figure S3	GC-MS spectrum of **1a** and **1c**.
Figure S4	a) Yields of 1c in different solvents; b) the influence of irradiation time on the amount of 1c; c) the PXRD of photocatalyst MOL **1**.
Figure S5	The TEM image for MOL **1** (a) and the morphology after reaction (b).
Figure S6	Isothermal adsorption/desorption curve of MOL **1**.
Figure S7-S13	^{1}H NMR spectra for **1c**~**1i**.
Figure S14	The calculated valence band hole (a) and conduction band electron (b) for MOL **1**.
Figure S15	The E_{ads} of species involved in synthesizing flavonoid by chalcone with MOL **1**.

Experimental Section

Materials and Measurements.

All reagents and solvents are commercially available (Beijing innoChem Science & Technology Co. Ltd.), and they were further dried by the vacuum rotary evaporator to remove all traces of water and then stored in the N_2-filled glovebox. The 15 mL Schlenk tube charged with a magnetic stirrer, which was used as the reactor (Scheme S1). The visible light (λ = 450 nm) was provided by a 30 W LED light.

Scheme S1. A photo of the reactor under 30 W LED light.

The chemical structures of the products were confirmed by comparison with standard chemicals and GC-MS (Agilent Technologies, GC 7890B, MS 5977A) data. GC equipped with a FID detector (Agilent Technologies, GC 7890 B) and a HP-5 5% phenyl methyl siloxane column (30m × 0.32mm × 0.5 μm), which was used for the quantifiable measure of flavonoid. ^{1}H NMR spectra was recorded on a Bruker UltraShield Plus Avance III (600 MHz). Peaks were referenced to residual solvent (DMSO). All products are tested after column purification.

A Varian Cary 500 UV-Vis spectrophotometer was used to record the UV-Vis diffuse reflectance spectra (DRS) of various solid samples. The photoelectrochemical characterization was performed on a Metrohm-Autolab AUT302N Electrochemical workstation. Photocurrent measurements were carried out in a typical three-electrode configuration with an Ag/AgCl electrode, a coiled Pt wire as the reference and counter electrode, respectively. X-ray diffraction (XRD) studies of catalyst were

carried out with a Bruker D8 Advance instrument. The electron paramagnetic resonance (EPR) experiments were carried out on Bruker A300 instrument operating in the X-band at room temperature.

Single-crystal X-ray crystallography.

Diffraction data for all complexes were measured on a Bruker SMART CCD diffractometer (Mo Kα radiation and λ = 0.71073 Å) in Φ and ω scan modes. All structures were solved by direct methods, followed by difference Fourier syntheses, and then refined by full-matrix least-squares techniques on F^2 using SHELXL.[1] All other non-hydrogen atoms were refined with anisotropic thermal parameters. Hydrogen atoms were placed in the calculated position and refined in the isotropic direction using a riding model. Table S1 summarizes X-ray crystallographic data and refinement details for the complexes. The CCDC reference number is 2189705 for MOL **1**. The coordination parameters of Dy(III) central coordination chemistry are completed by the *SHAPE* 2.0 program.[2]

Computational Studies

All computations were carried out using density functional theory (DFT)[3] implemented in Gaussian 09 suite of program.[4] Geometry optimizations were performed in the gas phase with M06-2X[5] levels of theory and 6-31G** basis set. After geometry optimizations, the energies were re-evaluated with optimized structures under M06-2X level and 6-311+G** basis set. Solvation energy corrections were carried out at the same level of the single point energy calculations using SMD[6] model (solvent = acetonitrile), where the solution phase electronic energies (E_{Sol}) were evaluated. Vibrational frequency calculations were conducted at the same level as the geometry optimizations, to derive the thermochemistry correction term (G − E) as well as to confirm the stationary points as either minima (no imaginary frequencies) or saddle points (one imaginary frequency) on the potential energy surface. Final solution phase Gibbs free energies (G_{Sol}) were computed as follows:

$$G_{Sol} = E_{Sol} + (G - E) \quad (1)$$

$$\Delta G_{Sol} = \Sigma G_{Sol} \text{ for products} - \Sigma G_{Sol} \text{ for reactants} \quad (2)$$

Synthesis of complex MOL 1.

Adding 37.6 mg H_2**L** ligand (0.1 mmol), and $Dy(NO_3)_3 \cdot 6H_2O$ (0.05 mmol) in 9 mL DMF and 1 mL H_2O, then stirred 30 minutes in 15 mL polytetrafluoroethylene reactor, the reactor was heated at 140 °C for 72 h. Then the reaction was terminated, the polytetrafluoroethylene reactor was cooled to room temperature, yellow strip crystals were obtained. The crystals were washed 2-3 times with DMF solvent for characterization and reaction. Yield: 76% (based on $Dy(NO_3)_3 \cdot 6H_2O$). Elemental analyses *calc.* (%) for $[Dy(C_{20}H_{10}N_2O_4S)2]_n \cdot (C_2H_8N)_n$: C 52.69, H 2.95, N 7.32. Found: C 52.74, H 3.01, N 7.29.

Table S1. Crystallographic data of the complex MOL **1**.

Complex	MOL **1**
Formula	$C_{42}H_{28}DyN_5O_8S_2$
Formula weight	957.31
T (K)	100.00 (10)
Crystal system	Triclinic
Space group	P-1
a (Å)	7.74310 (10)
b (Å)	13.8979 (2)
c (Å)	18.5548 (2)
α (°)	105.0820 (10)
β (°)	101.8790 (10)
γ (°)	91.5980 (10)
V (Å^3)	1879.64 (4)
Z	2
D_c(g cm^{-3})	1.691
μ (mm^{-1})	11.304
Reflns coll.	24315
Unique reflns	6637
R_{int}	0.0403
$^aR_1[I \geq 2\sigma(I)]$	0.0368
$^bwR_2$(all data)	0.0998
GOF	1.026

$^aR_1 = \Sigma||F_o|-|F_c||/\Sigma|F_o|$, $^bwR_2 = [\Sigma w(F_o^2-F_c^2)^2/\Sigma w(F_o^2)^2]^{1/2}$

Table S2. Selected bond lengths (Å) and angles (°) of complex MOL **1**.

MOL 1					
Bond lengths (Å)					
O5—Dy1	2.323 (3)	O8—Dy1^{ii}	2.352 (3)	O4—Dy1^{i}	2.451 (3)
O3—Dy1^{i}	2.557 (3)	O2—Dy1	2.533 (3)	O6—Dy1^{iii}	2.347 (3)
O7—Dy1^{i}	2.316 (3)	O1—Dy1	2.445 (3)		
Bond angles (°)					
O5—Dy1—O3^{iv}	159.15 (11)	O7^{iv}—Dy1—O1	146.37 (10)	O1—Dy1—O2	52.49 (10)
O5—Dy1—O8^{ii}	78.85 (10)	O7^{iv}—Dy1—O4^{iv}	75.39 (11)	O1—Dy1—O4^{iv}	130.27 (11)
O5—Dy1—O2	95.39 (10)	O7^{iv}—Dy1—O6^{iii}	76.68 (10)	O4^{iv}—Dy1—O3^{iv}	52.20 (10)
O5—Dy1—O1	77.07 (11)	O8^{ii}—Dy1—O3^{iv}	116.66 (10)	O4^{iv}—Dy1—O2	92.66 (10)
O5—Dy1—O4^{iv}	148.55 (10)	O8^{ii}—Dy1—O2	72.77 (10)	O6^{iii}—Dy1—O3^{iv}	75.44 (10)
O5—Dy1—O6^{iii}	92.56 (10)	O8^{ii}—Dy1—O1	116.46 (10)	O6^{iii}—Dy1—O8^{ii}	163.66 (11)
O7^{iv}—Dy1—O5	87.65 (11)	O8^{ii}—Dy1—O4^{iv}	74.63 (10)	O6^{iii}—Dy1—O2	122.30 (10)
O7^{iv}—Dy1—O3^{iv}	105.59 (10)	O2—Dy1—O3^{iv}	77.57 (10)	O6^{iii}—Dy1—O1	74.32 (10)
O7^{iv}—Dy1—O8^{ii}	89.00 (10)	O1—Dy1—O3^{iv}	83.22 (10)	O6^{iii}—Dy1—O4^{iv}	108.56 (10)
O7^{iv}—Dy1—O2	160.48 (10)				
Symmetry codes: (i) *x*+1, *y*, *z*+1; (ii) -*x*+1, -*y*+1, -*z*+1; (iii) -*x*+1, -*y*+1, -*z*; (iv) *x*-1, *y*, *z*-1.					

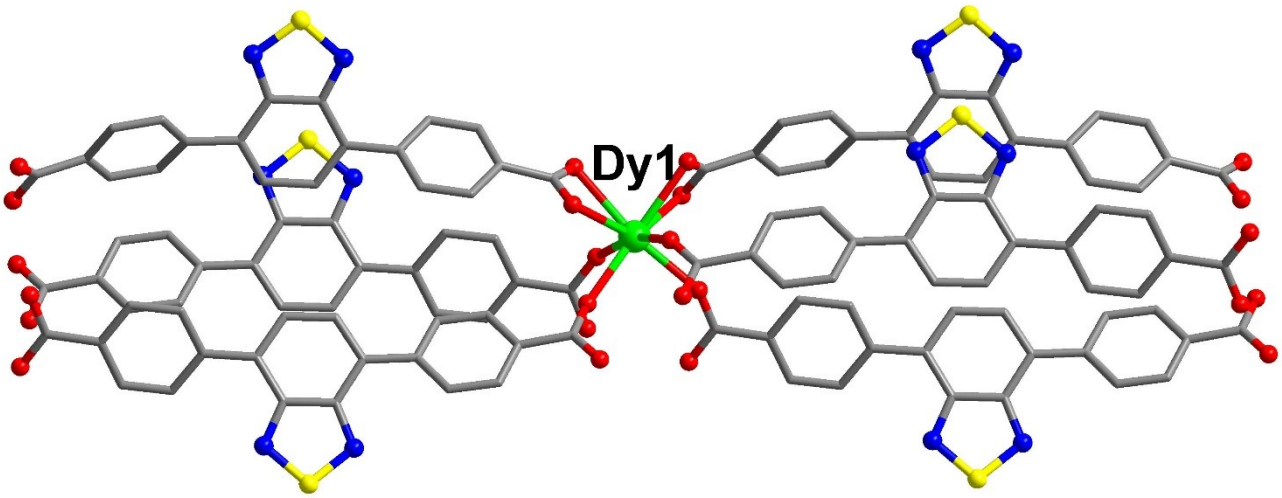

Figure S1. The coordinated environment of Dy(III) ion.

Table S3. *SHAPE* analysis of the Dy1 ion in MOL **1**.

Label	Shape	Symmetry	Distortion(°)
OP-8	D_{8h}	Octagon	34.914
HPY-8	C_{7v}	Heptagonal pyramid	22.286
HBPY-8	D_{6h}	Hexagonal bipyramid	12.267
CU-8	O_h	Cube	6.700
SAPR-8	D_{4d}	Square antiprism	3.368
TDD-8	D_{2d}	Triangular dodecahedron	2.707
JGBF-8	D_{2d}	Johnson gyrobifastigium J26	14.006
JETBPY-8	D_{3h}	Johnson elongated triangular bipyramid J14	27.248
JBTPR-8	C_{2v}	Biaugmented trigonal prism J50	4.471
BTPR-8	C_{2v}	Biaugmented trigonal prism	3.747
JSD-8	D_{2d}	Snub diphenoid J84	6.614
TT-8	T_d	Triakis tetrahedron	7.568
ETBPY-8	D_{3h}	Elongated trigonal bipyramid	23.374

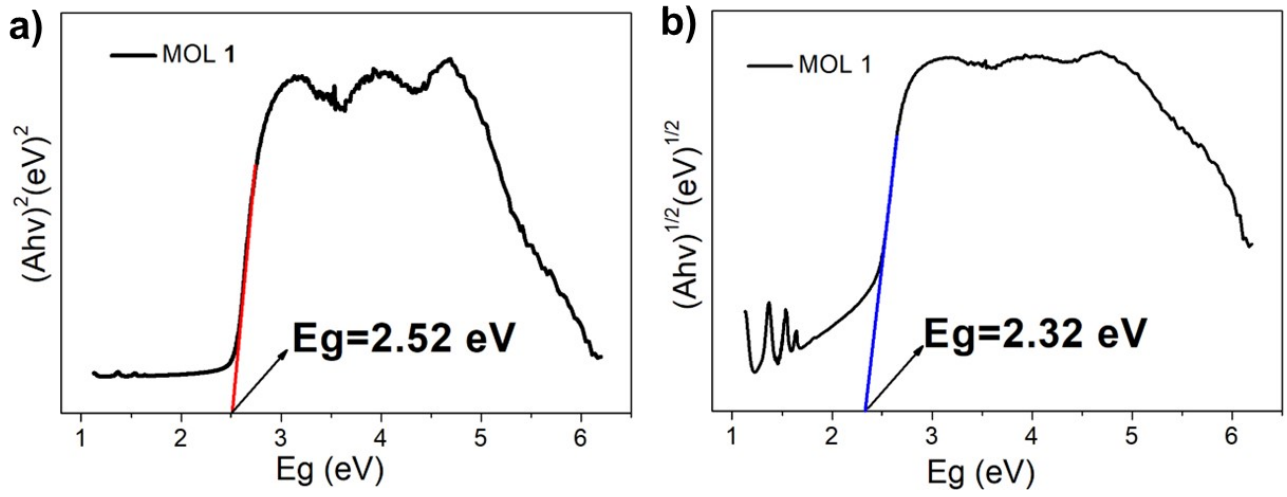

Figure S2. a) n = 2, the *Tauc* plot of MOL **1**; b) n = 1/2, the *Tauc* plot of MOL **1**.

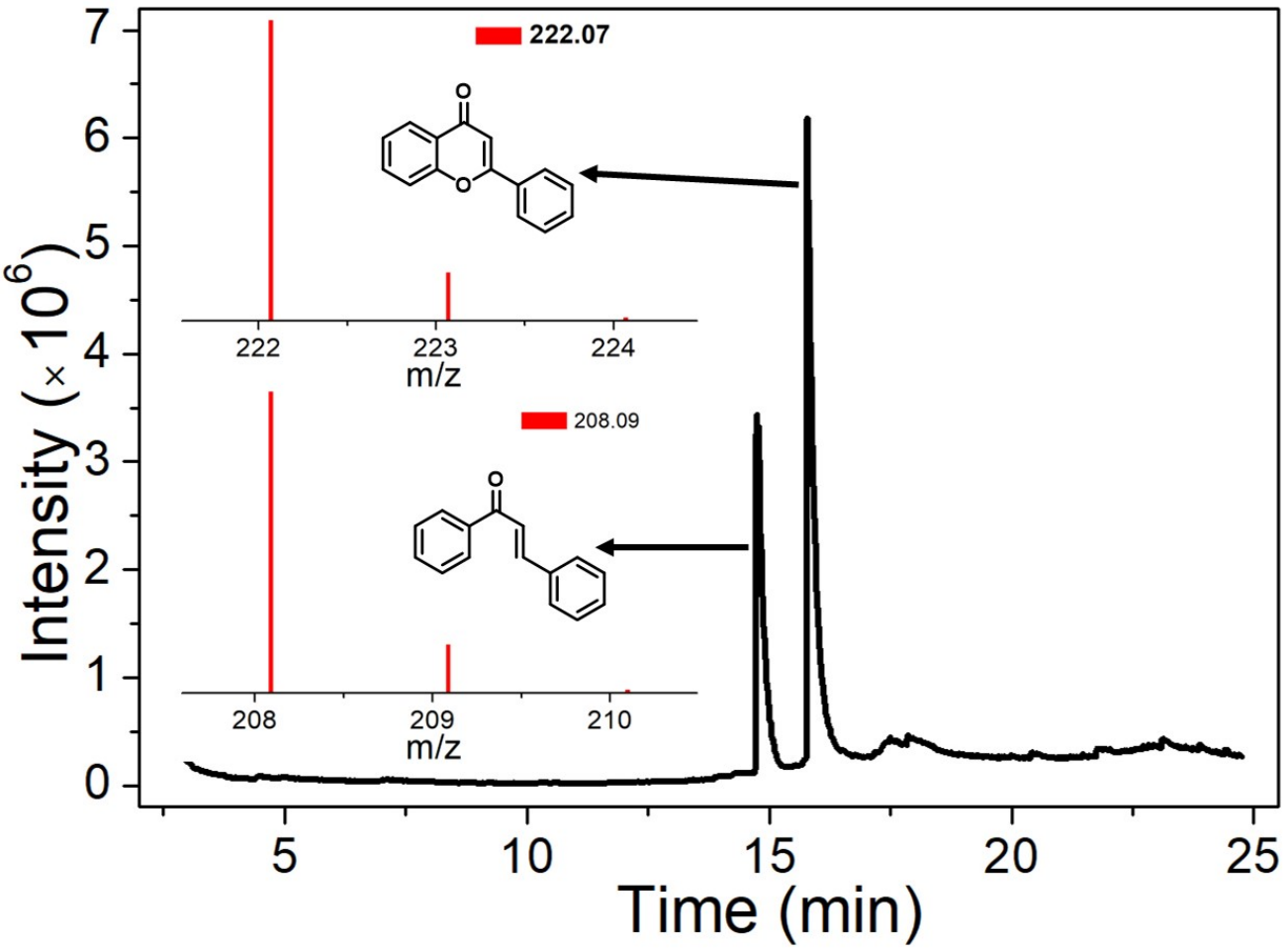

Figure S3. GC-MS spectrum of **1a** and **1c**.

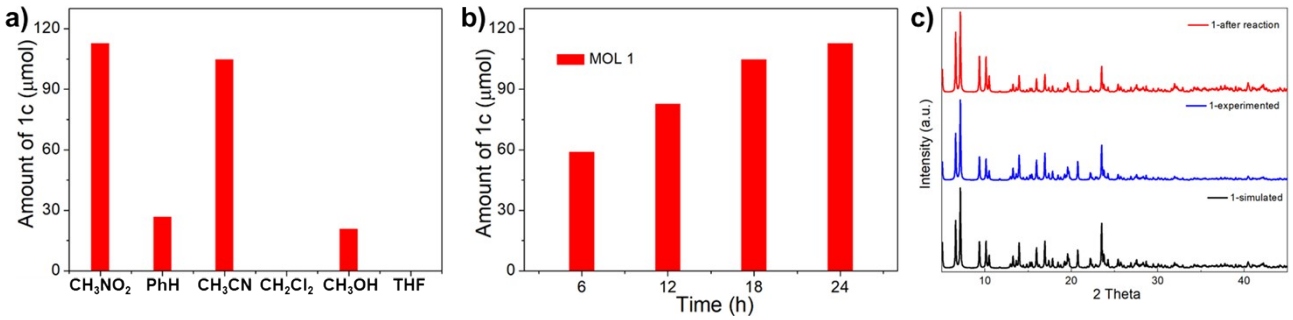

Figure S4. a) Yields of 1c in different solvents; b) the influence of irradiation time on the amount of 1c; c) the PXRD of photocatalyst MOL **1**. The PXRD data suggests that the MOL **1** is purity before reaction. After the reaction, only part of the peaks changed in height, and the peak position remained basically unchanged.

Table S4. Computed oxidation potential of chalcone.

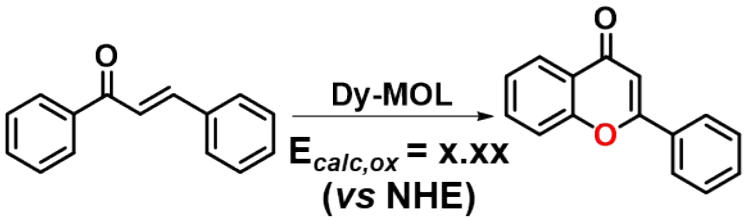

	$E_{calc,ox}$
E(NHE)	0.66

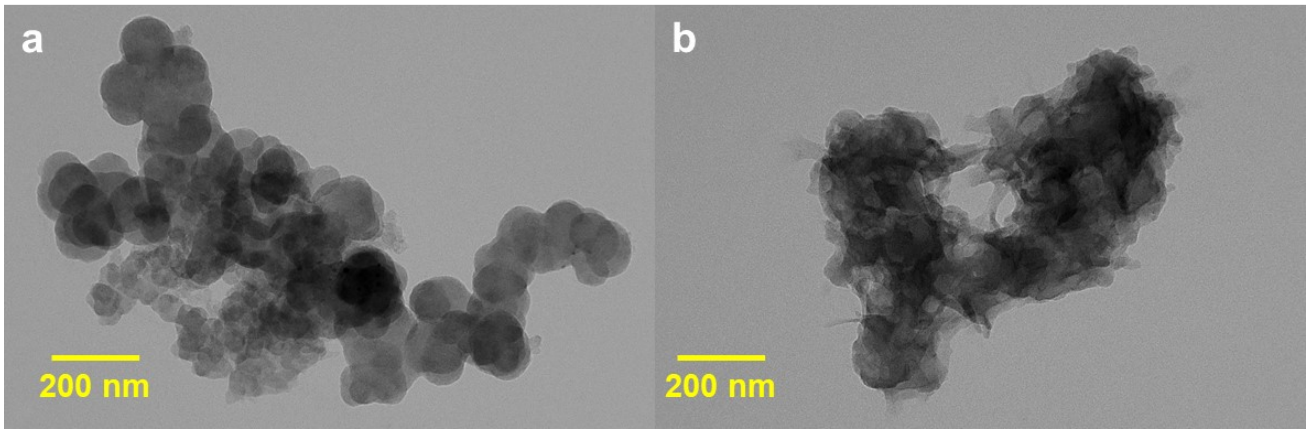

Figure S5. The TEM image for MOL **1** (a) and the morphology after reaction (b).

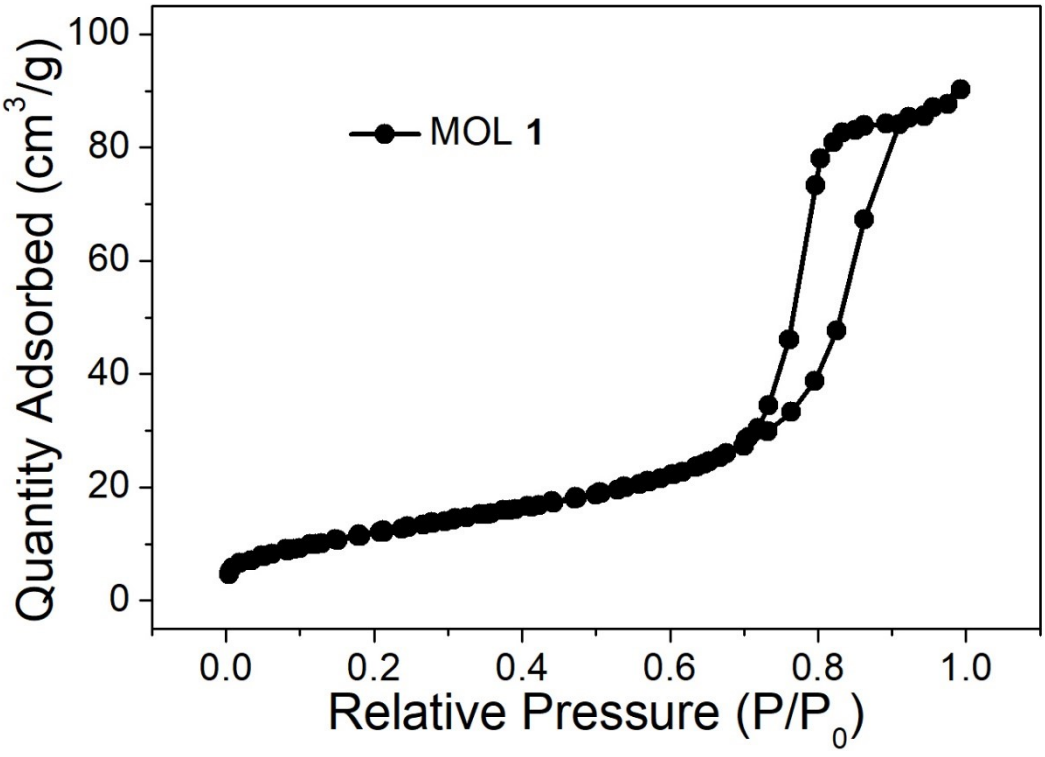

Figure S6. Isothermal adsorption/desorption curve of MOL **1**.

NMR Data:

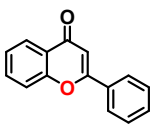

(**1c**): H NMR (600 MHz,) δ 8.23, 8.23, 8.22, 8.21, 7.93, 7.93, 7.93, 7.92, 7.92, 7.92, 7.92, 7.91, 7.91, 7.91, 7.91, 7.70, 7.70, 7.69, 7.69, 7.68, 7.68, 7.67, 7.57, 7.56, 7.55, 7.55, 7.53, 7.53, 7.53, 7.52, 7.52, 7.52, 7.52, 7.51, 7.51, 7.51, 7.50, 7.50, 7.50, 7.50, 7.49, 7.42, 7.42, 7.41, 7.41, 7.41, 7.40, 7.39, 6.83.

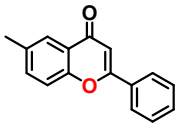

(**1d**): H NMR (600 MHz,) δ 8.01, 8.00, 8.00, 8.00, 8.00, 8.00, 7.92, 7.91, 7.91, 7.91, 7.91, 7.90, 7.90, 7.90, 7.53, 7.53, 7.52, 7.52, 7.52, 7.51, 7.51, 7.51, 7.51, 7.50, 7.50, 7.50, 7.49, 7.49, 7.49, 7.49, 7.49, 7.48, 7.46, 7.44, 6.81, 6.81, 2.45.

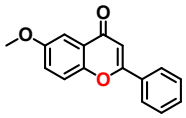

(**1e**): H NMR (600 MHz,) δ 7.91, 7.91, 7.91, 7.90, 7.90, 7.89, 7.59, 7.58, 7.52, 7.51, 7.50, 7.49, 7.48, 7.29, 7.29, 7.28, 7.28, 7.27, 7.27, 7.27, 7.25, 6.83, 6.82, 6.82, 3.90, 3.89.

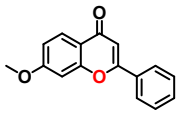

(**1f**): H NMR (600 MHz,) δ 8.13, 8.11, 7.90, 7.90, 7.89, 7.89, 7.88, 7.52, 7.52, 7.51, 7.51, 7.51, 7.50, 7.50, 7.25, 6.77, 3.92.

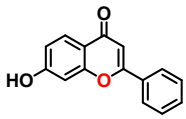

(**1g**): H NMR (600 MHz,) δ 11.88, 8.13, 8.12, 7.92, 7.91, 7.91, 7.91, 7.90, 7.90, 7.90, 7.89, 7.88, 7.53, 7.52, 7.51, 7.26, 7.26, 7.26, 7.26, 7.25, 7.25, 7.25, 7.25, 7.24, 7.24, 7.24, 7.24, 7.24, 7.24, 7.24, 6.77, 6.39, 6.32.

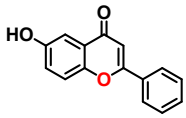

(**1h**): H NMR (600 MHz,) δ 9.93, 7.96, 7.95, 7.55, 7.25, 7.25, 7.25, 7.24, 7.24, 7.24, 7.24, 7.24, 6.77.

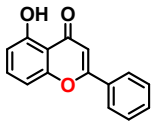

(**1i**): H NMR (600 MHz,) δ 7.91, 7.91, 7.91, 7.91, 7.90, 7.90, 7.90, 7.89, 7.89, 7.57, 7.57, 7.57, 7.56, 7.56, 7.56, 7.55, 7.55, 7.54, 7.54, 7.54, 7.53, 7.53, 7.52, 7.52, 7.52, 7.52, 7.51, 7.51, 7.51, 7.50, 7.25, 7.00, 7.00, 7.00, 6.99, 6.99, 6.98, 6.82, 6.81, 6.81, 6.80, 6.80, 6.80, 6.73, 6.73, 6.72, 6.72.

Copies of ^{1}H NMR spectra

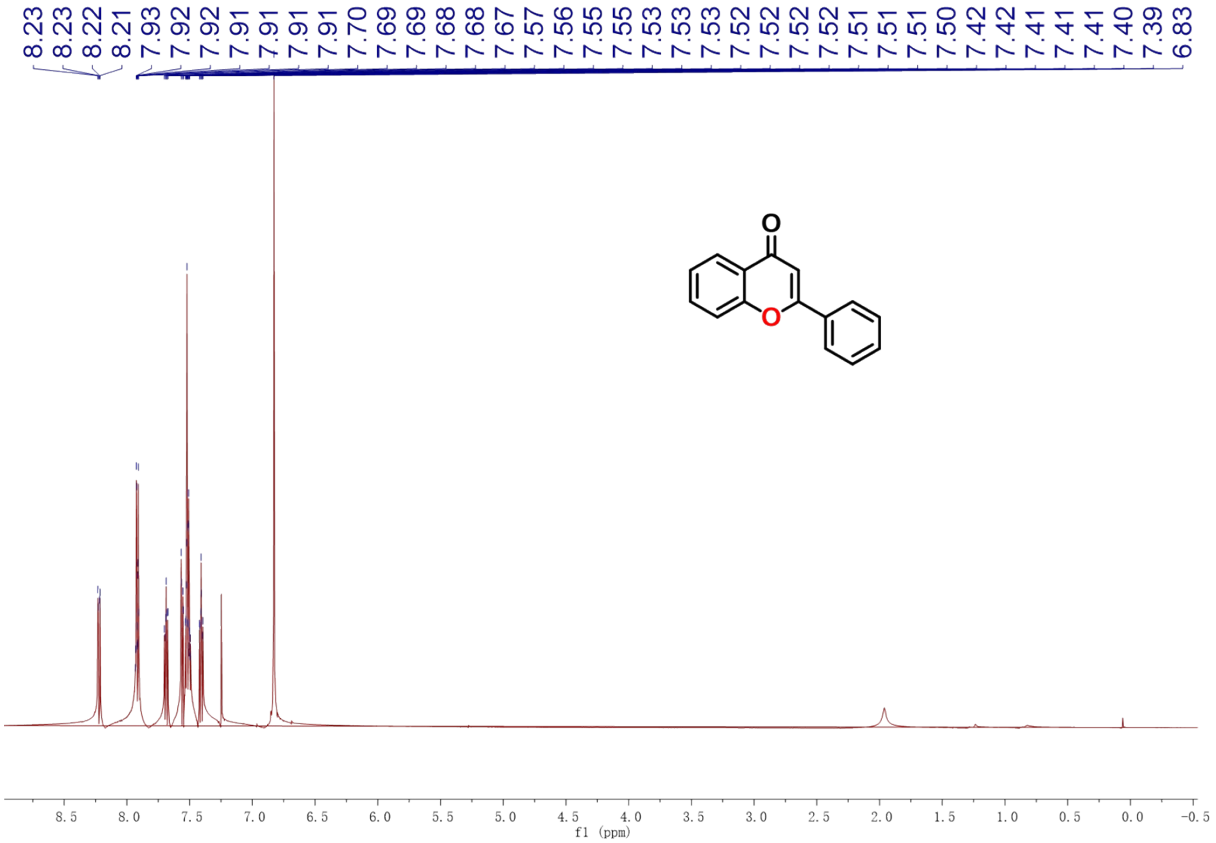

Figure S7. ^{1}H NMR spectra for **1c**.

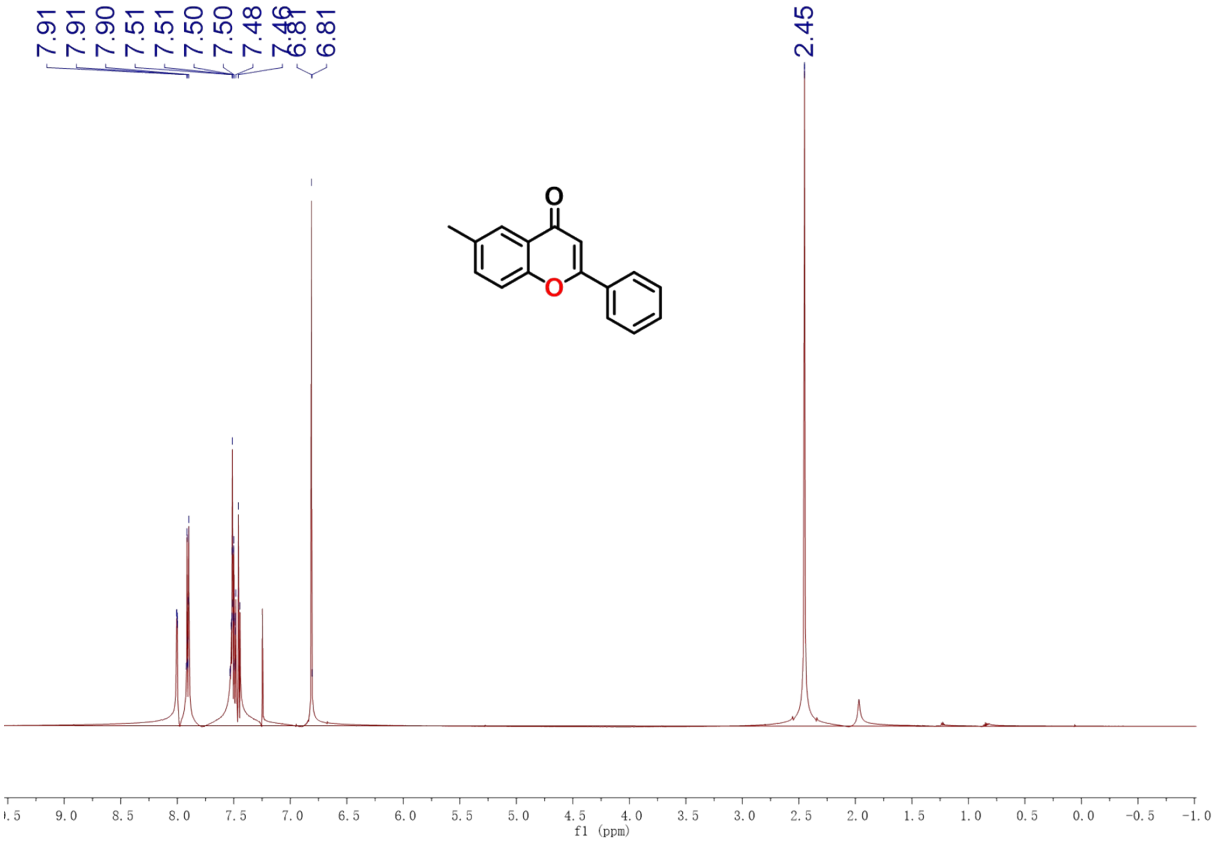

Figure S8. ^{1}H NMR spectra for **1d**.

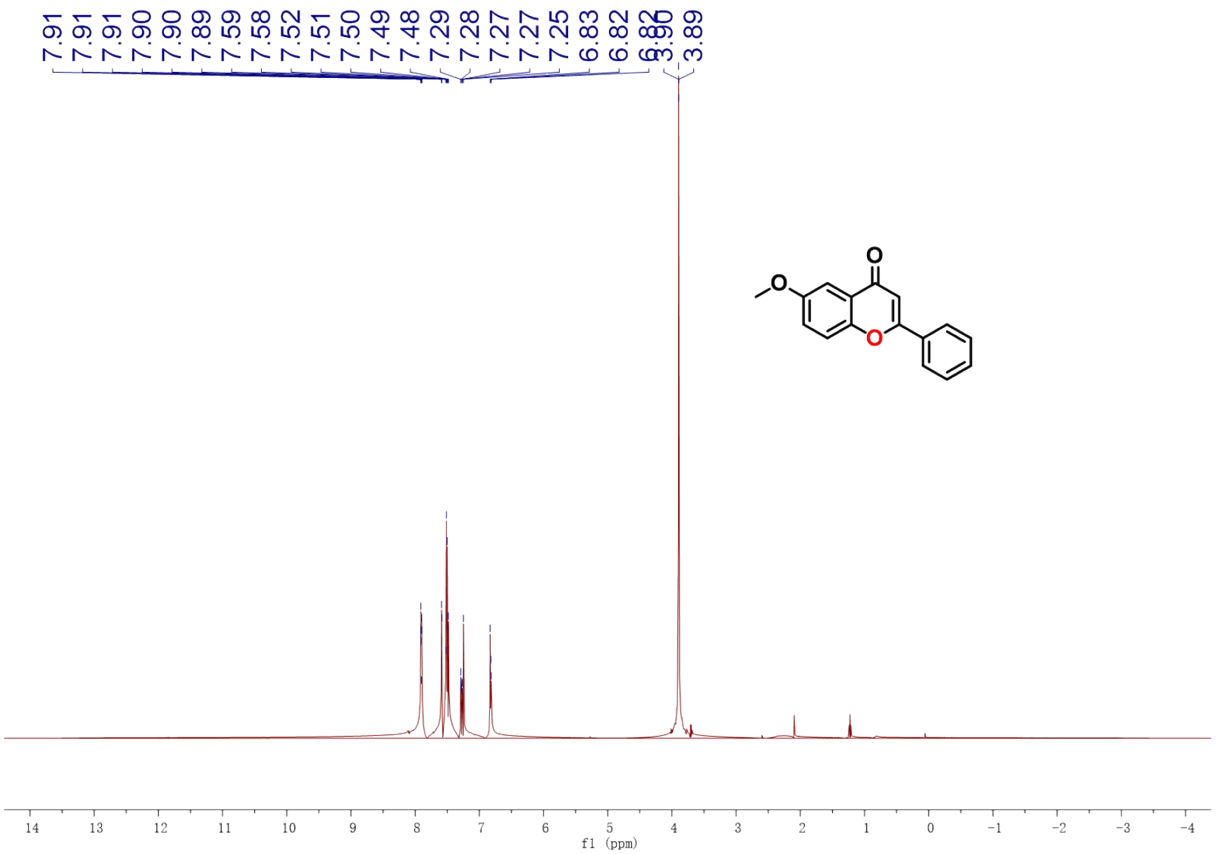

Figure S9. ^{1}H NMR spectra for **1e**.

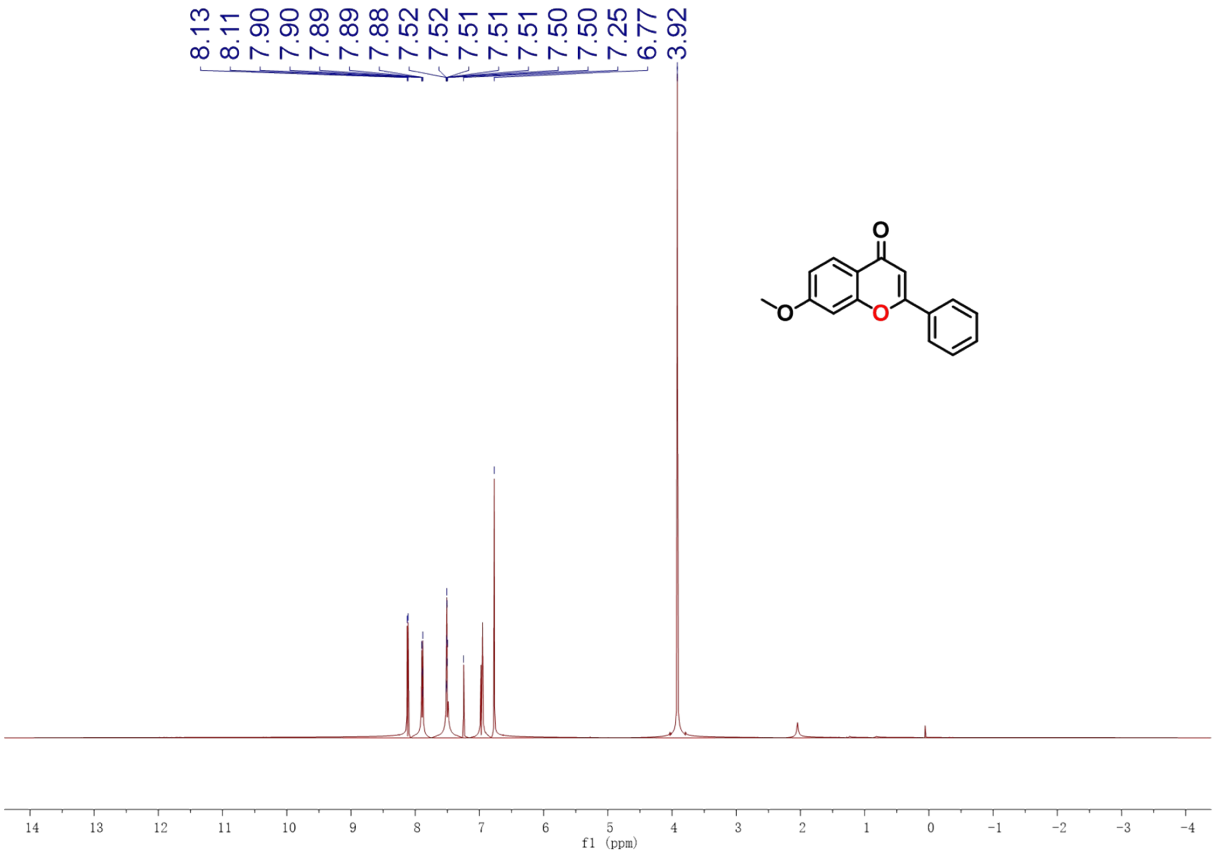

Figure S10. ^{1}H NMR spectra for **1f**.

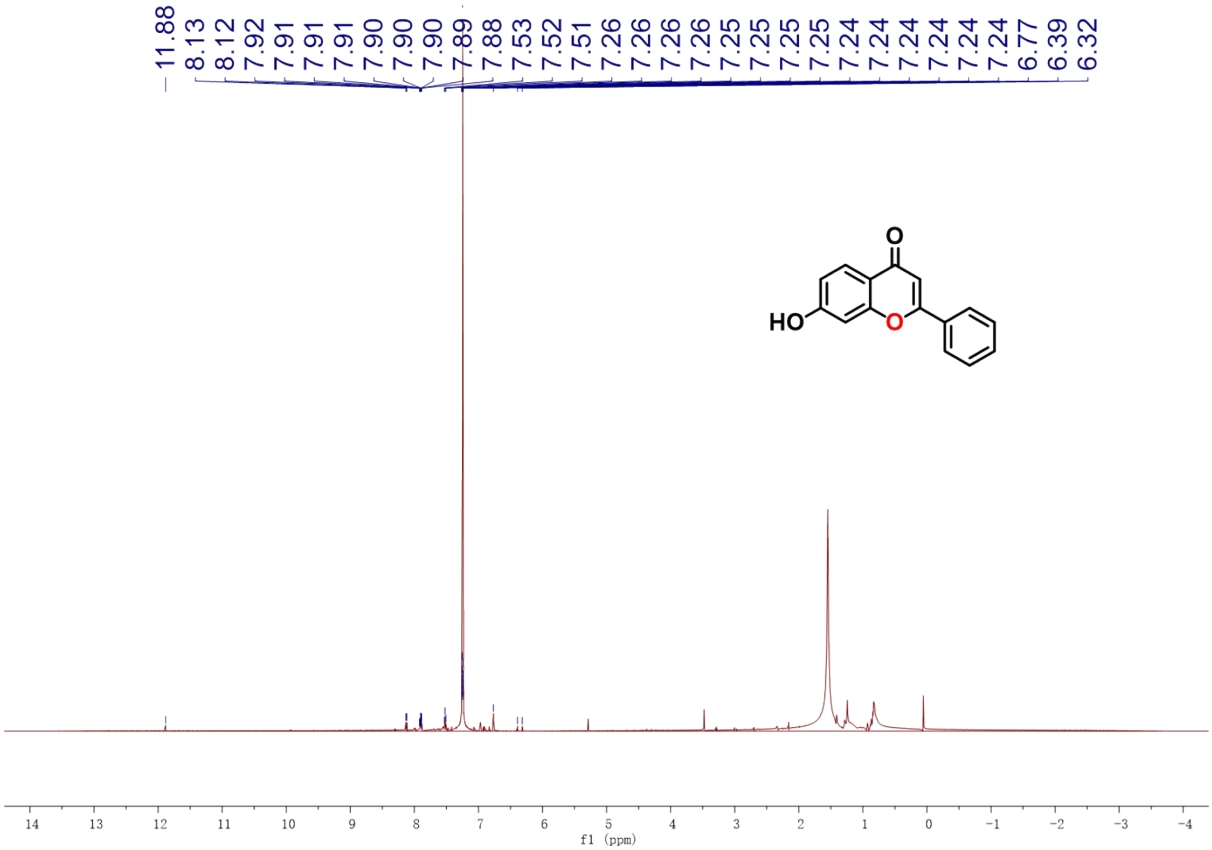

Figure S11. [1]H NMR spectra for **1g**.

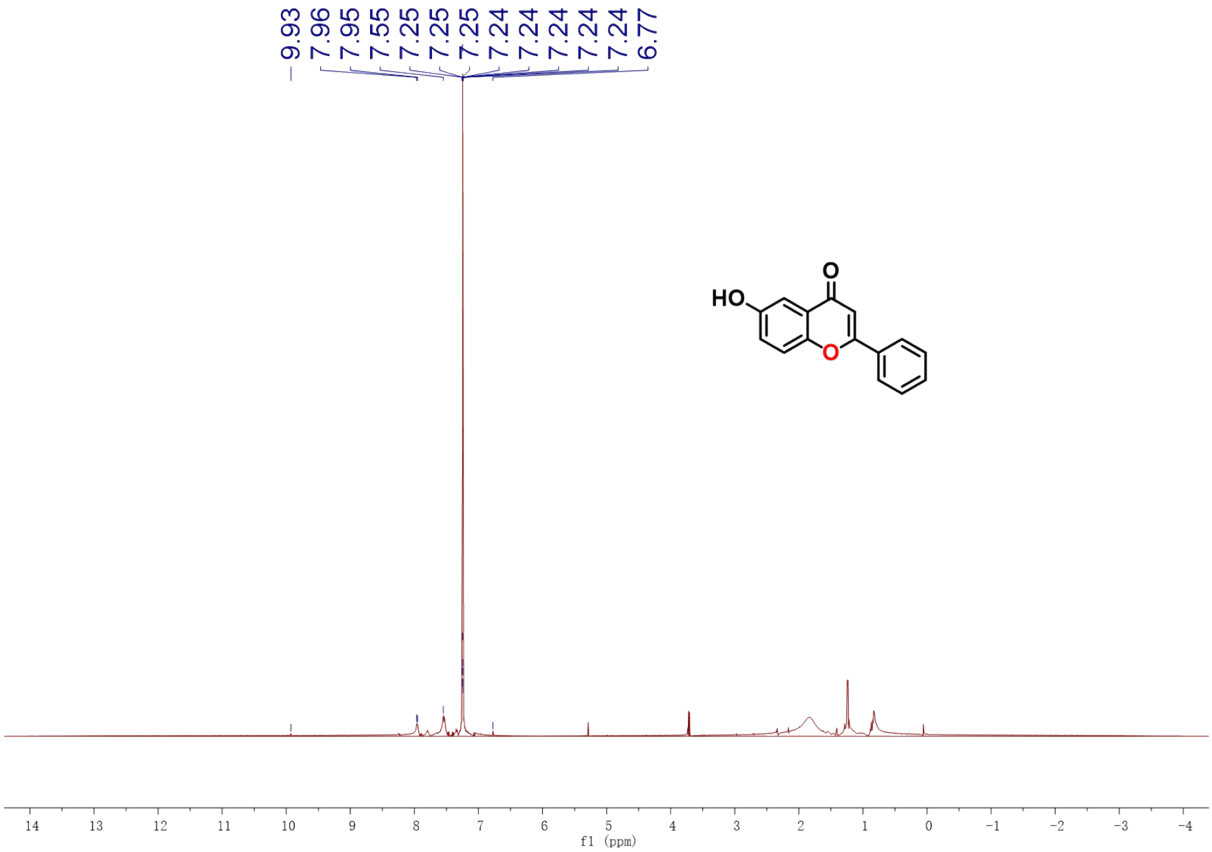

Figure S12. [1]H NMR spectra for **1h**.

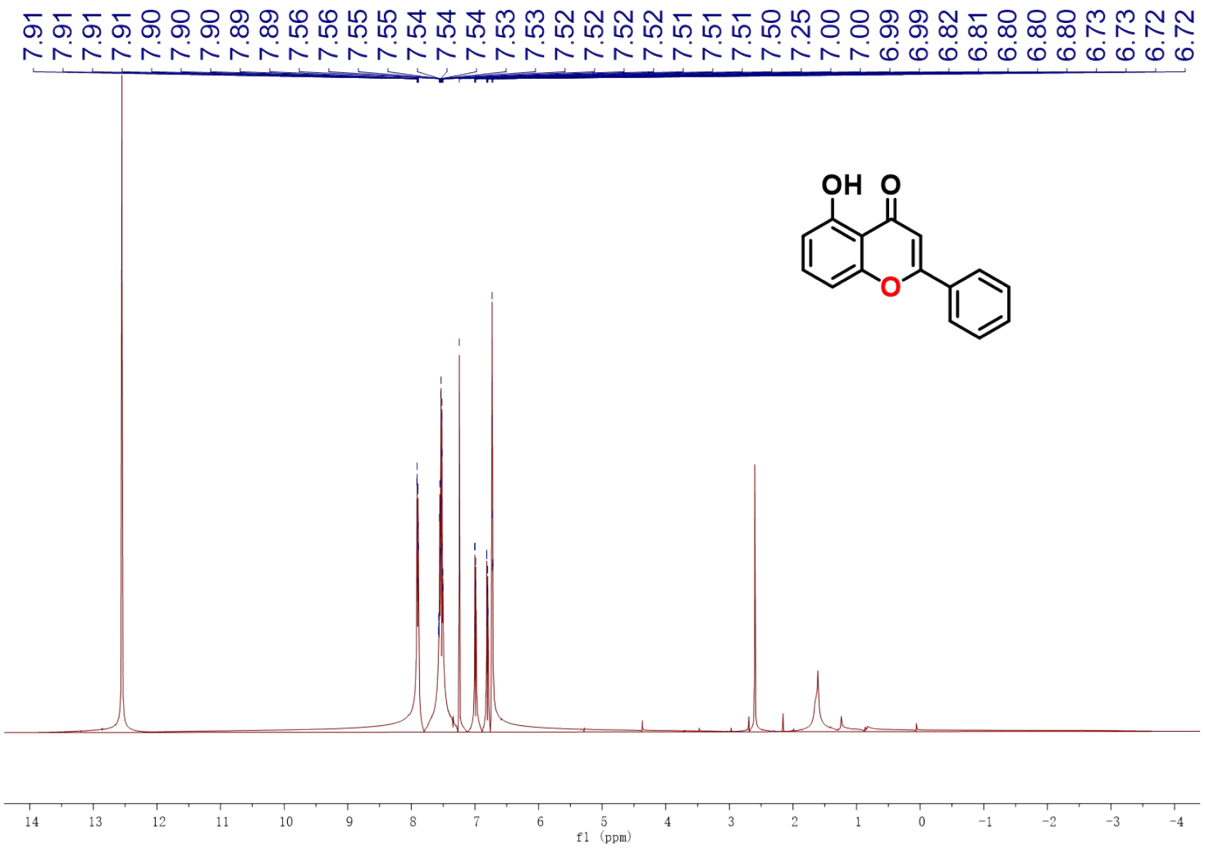

Figure S13. ^{1}H NMR spectra for **1i**.

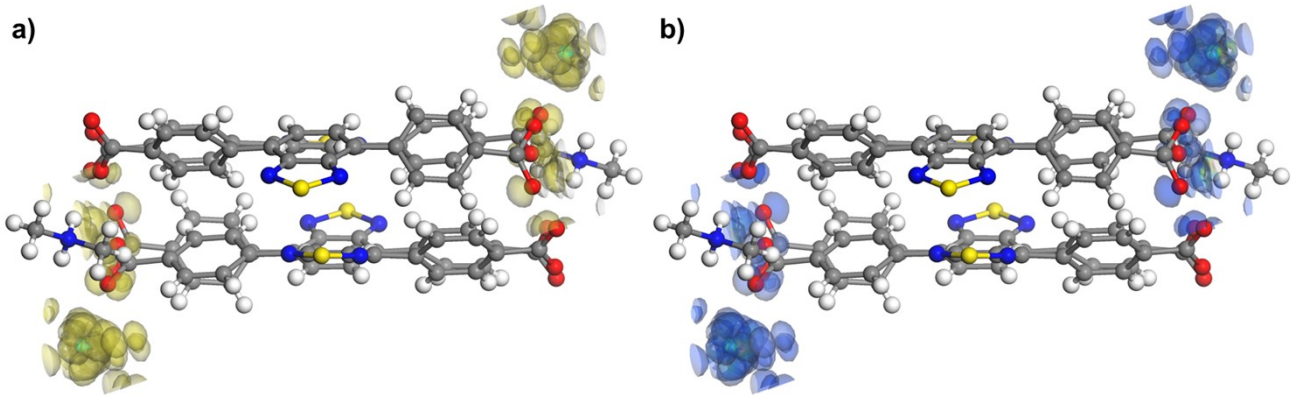

Figure S14. The calculated valence band hole (a) and conduction band electron (b) for MOL **1**.

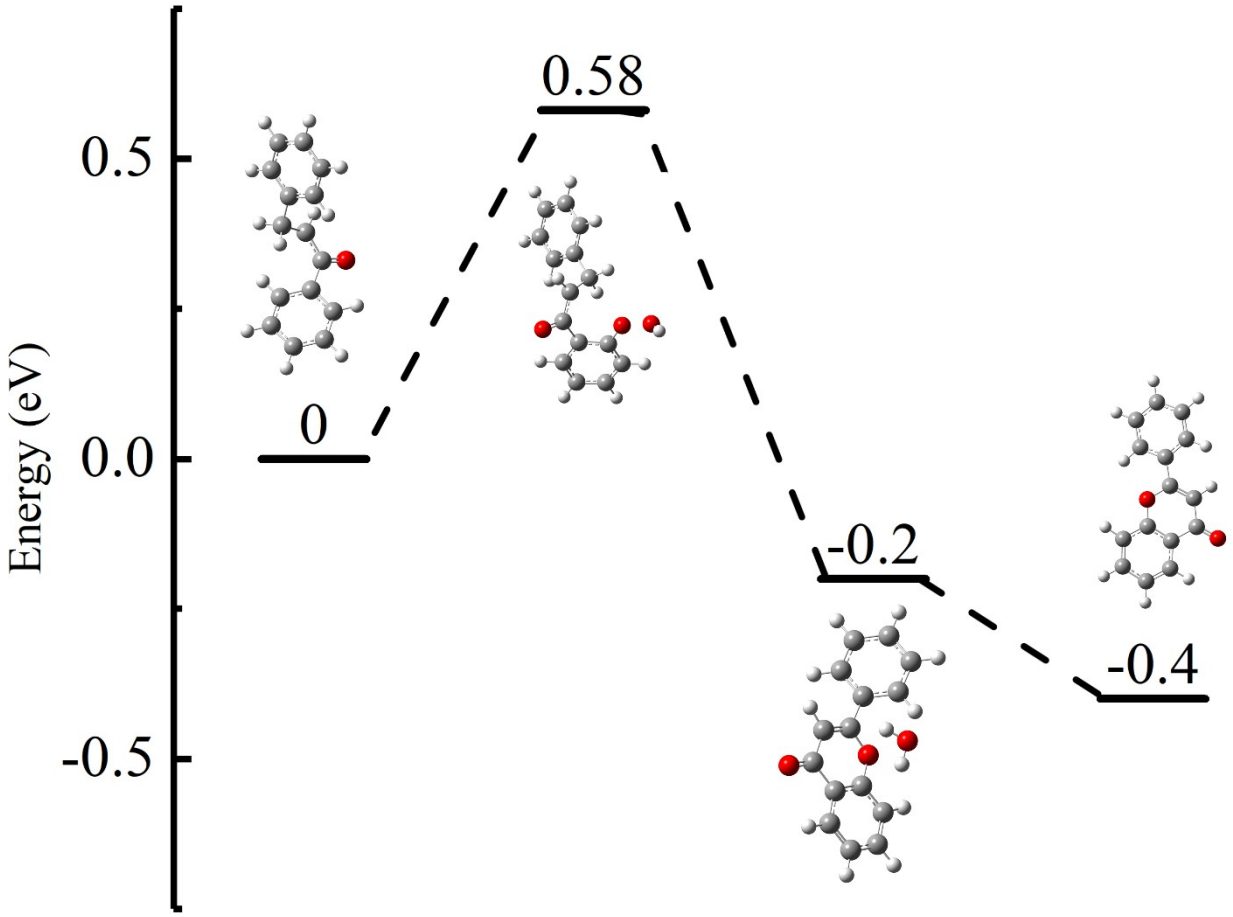

Figure S15. The E_{ads} of species involved in synthesizing flavonoid by chalcone with MOL **1**.

References.

1. G. M. Sheldrick, *Acta Crystallogr., Sect. C: Struct. Chem*. **2015**, *71*, 3-8.
2. S. Alvarez, P. Alemany, D. Casanova, J. Cirera, M. Llunell, D. Avnir. *Coord. Chem. Rev.,* **2005**, *249*, 1693.
3. R. G. Parr, W. Yang, Density-Functional Theory of Atoms and Molecules, Oxford University, Press, **1994**.
4. M. J. Frisch, G. W. Trucks, H. B. Schlegel, G. E. Scuseria, M. A. Robb, J. R. Cheeseman, G. Scalmani, V. Barone, G. A. Petersson, H. Nakatsuji, X. Li, M. Caricato, A. V. Marenich, J. Bloino, B. G. Janesko, R. Gomperts, B. Mennucci, H. P. Hratchian, J. V. Ortiz, A. F. Izmaylov, J. L. Sonnenberg, D. Williams-Young, F. Ding, F. Lipparini, F. Egidi, J. Goings, B. Peng, A. Petrone, T. Henderson, D. Ranasinghe, V. G. Zakrzewski, J. Gao, N. Rega, G. Zheng, W. Liang, M. Hada, M. Ehara, K. Toyota, R. Fukuda, J. Hasegawa, M. Ishida, T. Nakajima, Y. Honda, O. Kitao, H. Nakai, T. Vreven, K. Throssell, J. A. Montgomery, Jr., J. E. Peralta, F. Ogliaro, M. J. Bearpark, J. J. Heyd, E. N. Brothers, K. N. Kudin, V. N. Staroverov, T. A. Keith, R. Kobayashi, J.

Normand, K. Raghavachari, A. P. Rendell, J. C. Burant, S. S. Iyengar, J. Tomasi, M. Cossi, J. M. Millam, M. Klene, C. Adamo, R. Cammi, J. W. Ochterski, R. L. Martin, K. Morokuma, O. Farkas, J. B. Foresman, and D. J. Fox, Gaussian, Inc., Wallingford CT, **2019**.

5. Y. Zhao, D. G. Truhlar, *Theor. Chem. Acc*. **2008**, *120*, 215-241.
6. A. V. Marenich, C. J. Cramer, D. G. Truhlar, *J. Phy. Chem*. B **2009**, *113*, 6378-6396.